

On the motion of a fluid–fluid interface along a solid surface

By ELIZABETH B. DUSSAN V.†
AND STEPHEN H. DAVIS

Department of Mechanics and Materials Science,
The Johns Hopkins University, Baltimore, Maryland 21218

(Received 29 January 1973 and in revised form 6 February 1974)

A fluid–fluid interface that joins a solid surface forms a common line. If the common line moves along the solid, a mutual displacement process is involved and is studied here. Some simple experiments motivate the formulation of the basic assumption of the analysis. The basic assumption is a formalization of the idea that the fluid–fluid interface rolls on or unrolls off the solid. This forms an axiom for the mostly kinematical analysis that follows. The predictions are tested through a series of qualitative experiments. The role of the no-slip boundary condition at the solid surface is discussed.

1. Introduction

When an interface between two immiscible fluids joins a solid boundary, a line is formed. This line is sometimes known as the three-phase line or the contact line; in this study it is referred to as the *common line*.

Common lines have often been examined by physical chemists. Whenever the systems are viewed as continua, the theories applied are thermostatic and the configurations considered are in or near a static equilibrium. In thermostatics it is customary to model the interfacial region, i.e. the region between two immiscible fluids or between a fluid and a solid, as a smooth two-dimensional (non-Euclidean) surface imbedded in three-dimensional space. The surface is endowed with an energy per unit area. The system is said to be in thermostatic equilibrium if it is in a configuration of minimal energy. This requires that the Young–Dupré equation (Maxwell 1876) must be satisfied as long as the following three properties hold. (i) The interfacial energies per unit area vary smoothly. (ii) The surface of the solid is smooth. (iii) The solid is rigid. When applied to a two-dimensional system (of course, this also applies to three-dimensional systems) such as that shown in figure 1, this equation reads as follows:

$$\gamma_{12} \cos \theta_1 + \gamma_{1S} = \gamma_{2S}.$$

Here γ_{12} , γ_{1S} , γ_{2S} and θ_1 are the interfacial energies of the fluid–fluid interface, the fluid 1–solid interface and the fluid 2–solid interface, and the contact angle, respectively. While a good deal of experimental data has been compiled on

† Present address: Department of Chemical and Biochemical Engineering, University of Pennsylvania, Philadelphia, Pennsylvania 1917.

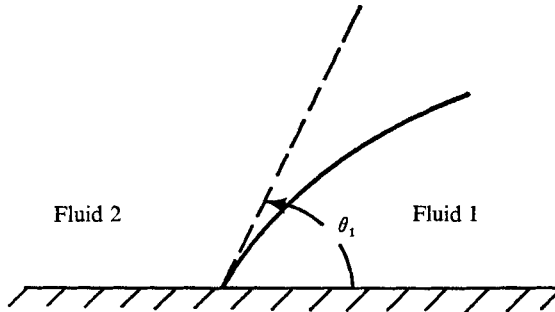


FIGURE 1. The region near the common line.

contact angles and interfacial energies at fluid–fluid interfaces for different combinations of materials, measurements of the interfacial energies at solid–fluid interfaces are of questionable validity (although see Read & Shockley 1950; Benson & Yun 1967). This means that the above model cannot be verified by substituting experimentally or theoretically obtained values of γ_{12} , γ_{1S} , γ_{2S} and θ_1 into the Young–Dupré equation and showing that it is satisfied. Hence, even from a *static* point of view the utility and correctness of this model for fluid–solid interfaces remain unclear. One direction of research taken by physical chemists is to use experimental measurements of θ_1 and γ_{12} as a means of deducing the molecular structure of solid surfaces (Zisman 1972). While such information is important for a complete understanding of the interfacial region, it does not seem to lead to a method of making predictions.

It is very curious that the *moving* common line has not received more attention from fluid mechanicians. There are numerous occurrences in which it plays an important role. The common line is central to the application of monolayer protective coatings to solid surfaces, and to the deposition of uniform liquid layers on paper in the manufacture of photographic film. In the latter case, knowledge of the maximum common-line speed without the entrainment of air would be valuable economically. The sloshing of a liquid in a partially filled container, the breaking up of a thin layer of liquid into beads on a solid surface, the flowing of rivulets, the type of splashing produced by a rock thrown into a pail of water (Worthington 1963), and the flowing of a drop of dew down a blade of grass are further examples. In addition, the operation of transducers such as depth meters, used for measuring the amplitudes of small waves on liquid surfaces, depends directly on the motion of a common line since their operation hinges on how much of them is momentarily submerged in the liquid. Here the shape of the meniscus and the velocity of the common line are of great interest.

However, the problem is at present at a primitive stage. One cannot merely pose and solve a boundary-value problem which contains a free surface since at this point it is not even clear what boundary conditions should be imposed in the neighbourhood of the moving common line. One difficulty arises with the no-slip condition. It is frequently thought that there is an inherent contradiction in simultaneously assuming the no-slip boundary condition at a solid wall and expecting one fluid to displace another fluid there. In other words, the flow field

associated with the moving common line is thought to be incompatible with the no-slip boundary condition. As a result, in many situations in which the common line is important, devices are used to *avoid* analysing the flow field in the immediate neighbourhood of the common line.

In an investigation made by Ludviksson & Lightfoot (1971) of a thin film spreading up the sides of a vertical non-isothermal plate partially submerged in a pool of squalane, it is stated that, owing entirely to the no-slip condition between the liquid and solid wall, hydrodynamics cannot describe the flow in the neighbourhood of the leading edge of the fluid. Therefore, the leading edge must advance by diffusional processes. However, in their analysis, the diffusional process is ignored because it is poorly understood and an *ad hoc* technique is used to extend the analysis up to the leading edge of the liquid film. In an earlier article (Ludviksson & Lightfoot 1968) the rise of a column of liquid in a capillary tube is investigated. Here again the flow at the leading edge is not investigated; the analysis at most applies to the thin film of liquid at the wall of the capillary near the leading edge. (This, of course, assumes that there exists such a thin region.)

Prutow & Ostrach (1971) have studied the movement of the interface formed by one fluid displacing a second fluid in a capillary tube. The theory is limited to receding interfaces having small contact angles. Their asymptotic analysis divides the flow field into an inner and outer region. The inner domain consists of a three-phase region together with an adsorbed (deposited) film on the tube wall. This thin film is modelled as a three-dimensional Newtonian fluid. This adsorbed layer is assumed present so that the whole problem of one viscous fluid displacing another at a solid wall is avoided.

Hansen & Toong (1971) have investigated the mutual displacement of two immiscible fluids in a circular capillary tube. An incorrect demonstration of the existence of a discontinuity in one of the velocity components is given; it is assumed that the tangential component of the velocity of the fluid at points on the fluid–fluid interface is the same as the common-line speed. This is not necessarily true. Physical reasons are given why the ‘classical concepts of fluid mechanics and surface physics do not satisfactorily describe the solid–fluid–fluid intersection region’. As a consequence of these arguments the flow field in a ‘vicinity’ of the common line is analysed but the fluid within a distance δ of the common line ($\delta \approx 10^{-5}$ cm) is excluded from consideration. The analysis assumes that both fluids are Newtonian, that there is no slip at the rigid walls, that the velocity field is continuous across the fluid–fluid interface, and that there is a jump in the stress tensor at the fluid–fluid interface solely due to surface tension. The problem is then solved numerically. It is found that the curvature of the fluid–fluid interface is large at a distance δ from the wall of the tube, so that the tangent to the interface is undergoing rapid changes near the wall. This result leads Hansen & Toong to suspect reported experimental values of the dynamic contact angle. The analysis presumes that the speed of the common line and the tangent of the fluid–fluid interface at a distance from the wall are known.

A first attempt to deal theoretically with the moving common line was made

by Huh & Scriven (1971). The geometry is simplified somewhat by assuming the bounding wall to be rigid and planar. In addition, the motion in the neighbourhood of the common line is assumed to be describable by the two-dimensional, steady, constant density Navier–Stokes equations subject to the Stokes approximation (creeping flow). The *fluid–fluid interface is assumed to be planar*. An analytical solution to the associated boundary-value problem is attempted but in a strict sense no solution is found owing to their inability to satisfy the condition of continuity of the stress tensor across the fluid–fluid interface. Furthermore, the velocity field obtained has the property that the fluid exerts an *infinite force* on the bounding surface at the common line. Their analysis generalizes Moffatt's (1964) from a vacuum–fluid system to a fluid–fluid one.

Huh & Scriven clearly realize the deficiencies of the analysis but are unable to pinpoint the *cause* of the defects because their model imposes several strong restrictions on the problem, *a priori*.

Bascom, Cottington & Singleterry (1964) have looked at the problem of a moving common line experimentally. The lower edge of a vertical plate is immersed in a pool of squalane. Using interferometric techniques, the thickness of the thin film of squalane is measured as it climbs up the plate. A 'very' thin film, which *precedes* the leading edge and is referred to as a primary film or foot, is found. This film is detected by blowing water vapour onto the surface, and by the motion of minute drops of a liquid with a higher surface tension than squalane placed on this 'invisible' film. The foot cannot be detected by an ellipsometer for the first few hours. However, after 18 h, quantitative measurements show a foot several millimetres along and less than 50\AA thick. The existence of the foot is reported to be due to surface diffusional processes and not to evaporation–condensation. The nature of this process is not explained.

Schonhorn, Frisch & Kwei (1966) investigated experimentally the spreading of polymer melts on aluminium and mica surfaces. A small drop of a polymer (polyethylene and ethylene–vinyl acetate) is placed on a horizontal surface and observed for about one hour. It is found in all cases that, as the drop spreads, its configuration follows very closely that of a spherical cap. No thin film or 'foot' preceding the drop on the surface can be detected to within $10\mu\text{m}$ of the 'apparent' leading edge.

The purpose of the present study is threefold. (i) By way of simple qualitative experiments, the general nature of the motion of the fluids in the vicinity of a moving common line will be displayed. It will be seen that one fluid undergoes a 'rolling' type motion (§ 2), while the motion of the other fluid is more intricate. This involves fluid very close to the solid wall (or the fluid–fluid interface) being transported into the interior of the fluid (§ 3). (ii) The observations of the qualitative experiments will be combined with assumptions often made in fluid mechanics and it will be shown that the difficulties which have been encountered, when attempting to solve specific boundary-value problems, are a direct consequence of the continuum modelling (§§ 4 and 5). The difficulties are not a consequence of the particular approximate mathematical techniques used. (iii) It will also be shown that the no-slip boundary condition and the moving common line are kinematically compatible concepts (§ 3).

In the process of establishing (ii), the point of view taken is that there are certain features common to whole classes of such motions associated with the moving common line, which necessarily give rise to flow fields with certain general properties. In the following sections some of these properties will be derived. In order to do this no assumptions will be made about the position or shape of the fluid–fluid interface. The history of interfacial research is plagued by contamination of experimental interfaces and the elaborate modelling of interfaces by theoreticians. The properties which will emerge here are *independent of the structure endowed to any of the interfaces* (e.g. constant or variable surface tension, surface viscosities, surface elasticities, etc.). In most of the work, no *constitutive equation* (a relation between stress and other variables) *for the bulk fluids will be imposed*, so that the derived properties of the motion will be characteristic of Newtonian as well as non-Newtonian fluids. In fact, in most of the work the balance of linear momentum will not be used. In several parts of the analysis, the wall shape is not imposed, so that roughness is not excluded. In this study the existence of a foot preceding the common line is not excluded. If the foot exists, has properties and moves forward as a bulk, it, itself, has a front and so a common line. The work done here would apply to this configuration. If the foot exists as a result of surface diffusion and can be modelled as a ‘surface fluid’, the properties of the interface would be modified. But, no assumption concerning the properties of the interface is made in the analysis so that such an occurrence is likewise included herein.

2. The basic assumption of the model

The problem of the rise of water in a partially immersed capillary tube is a classical one discussed in elementary physics books. The final height is predicted by balancing the vertical component of the surface-tension force at the common line (air, water, glass) with the weight of the water column. Implicit in this analysis is the assumption that the water makes contact with the inside of the tube although it safely may be said that molecules of air as well might well be found on the water–solid interface. This assumption is reasonable since the resulting prediction is in good agreement with experiment. Further, a molecular model of the trapped air would scarcely lead to a tractable model for predicting the water column height.

The fluid flow in a neighbourhood of a *moving common line* will be examined in the same spirit. A basic assumption in the analysis to follow is first posed.

A common line is understood to be the intersection of the interface, which divides two mutually displacing materials, with the surface of a solid bounding wall. The two displacing materials will be referred to as fluids; the name does not imply any restriction on the form of their constitutive equations relating stress to the other variables. In the same way, the bounding wall is called a solid. For brevity, the *displaced* fluid will be called F_1 , the *displacing* fluid will be called F_2 and the solid will be called S . The three interfaces that meet to form the common line (CL) will be called SF_1 , SF_2 and F_1F_2 .

Basic assumption of the moving-common-line model. In a *finite* interval of time

either (a) material points on F_1F_2 are mapped (forward) onto CL , or (b) material points on CL are mapped (backward) onto F_1F_2 . The terms forward and backward are introduced to make later reference easy.

Implicit in the basic assumption is the notion that material points either arrive at the wall and *make contact* or *leave the wall* after having been in contact. None of F_1 'leaks' under F_2 onto SF_2 . It must then be plausible, as in the case of the capillary tube rise, to exclude the existence of a lubrication layer (bulk material) of F_1 between F_2 and S . It is emphasized that this model is not suggested for *any* two fluids and solid since not all combinations of such materials exhibit moving common lines.

The distinction between a lubrication layer and the presence of only a 'few' molecules is illustrated in a 'popping' drop experiment. Let us release a 0.1 cm³ drop of water into a horizontal tank containing silicone oil. The water drop contains food dye for visual purposes. The drop remains relatively spherical as it falls and appears, to the naked eye, to be fairly spherical for 5–10 s while it rests at the 'bottom' of the tank. All of a sudden the drop of water 'pops' on the Plexiglas base and achieves an entirely different configuration; refer to figure 2 (plate 1). When the drop reaches the bottom and appears to be at rest, it is not actually in contact with the Plexiglas; a slowly draining lubrication layer separates the drop from the Plexiglas base. After this layer of oil has reached some critical thickness, a drastic change in configuration of the drop suddenly occurs; the drop 'pops' down onto the solid, enlarging its area of apparent contact and displaying a distinct contact angle at its margin. It seems reasonable to analyse the 'popped' drop by assuming direct contact between the water and the Plexiglas (physical chemists would in contact-angle studies) rather than, say, using a Navier–Stokes theory for the 'trapped' molecules of oil.

A more detailed view of the 'popping' phenomenon can be obtained by using a glycerine drop (about 1500 times more viscous than water) to slow down the process. Figure 3 (plate 2) shows the popping process as a curve dividing two distinct types of reflexions. This curve seems to appear after an initial rupture of the lubrication layer and then sweeps across the lower surface of the drop. It is this change in the reflexion of light that serves to distinguish *functionally* the lubrication-layer case from the contact case. Simple experiments with moving common lines allow the same kind of decision.

The above discussion cannot exclude the existence of F_1 molecules on SF_2 but only makes plausible our model of continua F_2 and S in contact. In a practical sense, a molecular layer of F_1 can make its presence felt by altering the interfacial energy of SF_2 . This is allowed in the present analysis.

The explicit statement of the basic assumption is now examined. Four experiments will now be described which demonstrate qualitatively that, in finite times, material points are either mapped from CL to F_1F_2 or to CL from F_1F_2 . All the experiments illustrate the basic assumption for various cases. In (i), a liquid displaces a gas (forward); in (ii), a gas displaces a liquid (forward); in (iii), a liquid displaces a liquid (forward); in (iv), a liquid displaces a liquid (backward). Thus, a whole class of systems possessing moving common lines is within the realm of the present analysis.

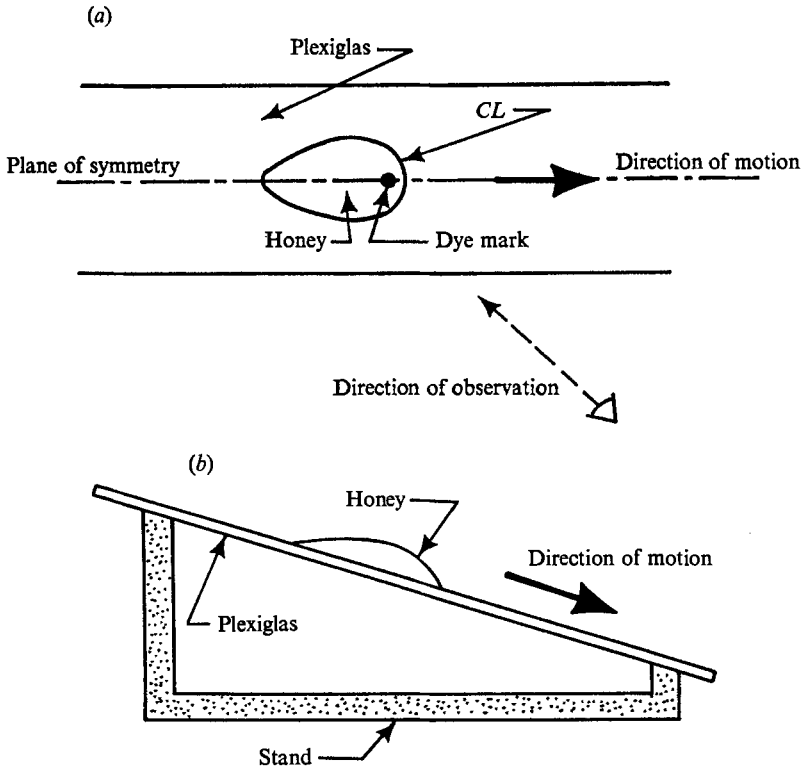


FIGURE 4. (a) Plan view and (b) side view of a drop of honey on a Plexiglas surface.

(i) Let F_1 be air, F_2 be honey, S be Plexiglas and consider a ‘forward’ configuration. About 1 cm^3 of honey is placed on a horizontal Plexiglas surface. A small dye mark, which consists of a honey and a McCormick’s food dye mixture, is placed by means of a sewing needle on the air–honey interface at the plane of symmetry of the honey; see figure 4 (a).

The dye mark appears initially to be circular and slowly tends to increase in size possibly owing to a surface-tension gradient induced by the presence of the food dye. The Plexiglas is tilted and the honey starts moving downward (see figure 4b). The trajectory of the dye mark is photographed from the direction indicated in figure 4 (a). The camera is inclined at a slight angle, pointing down towards the drop. As a consequence of the downward tilt of the camera, a mirror image of the drop on the Plexiglas surface can be seen. The common line can be located by viewing along the line formed by the intersection of the honey–air interface with its reflected image; see figure 5 (a) (plate 3). As the honey moves forward, so does the dye mark. Throughout, the dye mark roughly retains its circular geometry. Finally, in figure 5 (c) the dye mark seems to make contact with the Plexiglas, and therefore constitutes part of the common line. In figure 5 (d), more than half of the dye appears to be in contact with the Plexiglas surface and the remaining part is still on F_1F_2 ; the reflected image of this latter portion makes the mark appear to be a small dark spot. Figure 5 (e) shows no dye mark

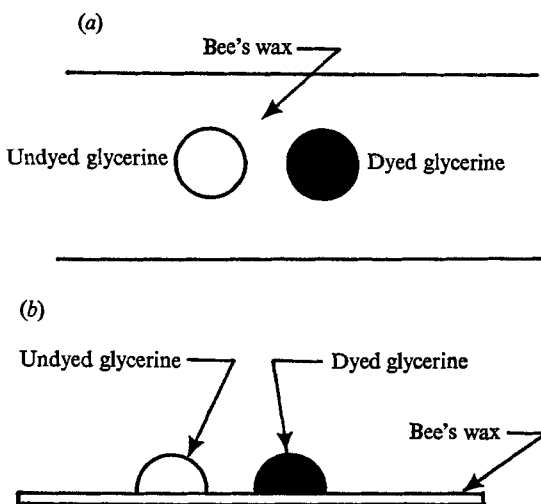


FIGURE 6. (a) Plan view and (b) side view of two drops of glycerine. One drop is dyed, the other is transparent.

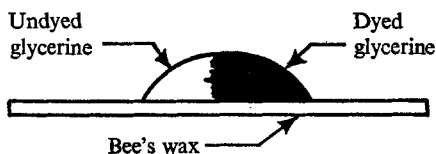


FIGURE 8. Cross-sectional view of a drop of glycerine which is partially dyed.

at all. The spot can then be seen from above. The part apparently in contact with the Plexiglas remains adhered while the portion of the spot not in contact gets sheared by the honey flow.

It is important to note that the dye mark does not spread out in the direction parallel to the Plexiglas surface as it approaches the common line. Material points on F_1F_2 have been observed. That is, those points of material (honey) marked by the dye and which also lie on the interface (such points probably exist since there is a tendency for the dye mark to grow in size) follow a trajectory which brings them to the common line in a finite length of time.

(ii) Let F_1 be glycerine, F_2 be air and S be bee's wax. The surface is prepared by pouring molten wax into a dish and letting it solidify and cool to room temperature. A definite crystalline structure can be observed. Two drops of glycerine, one transparent and the other dyed (with McCormick's food dye) are placed side by side on the wax surface; see figure 6. The wax surface is tilted from the horizontal, causing the right end to be lower than the left end. After a very short time, the two drops merge, whereupon the solid surface is made horizontal again; see figures 7(a) and (b) (plate 4). A cross-sectional side view would probably look like figure 8. Only *one* drop of glycerine is now present; it has approximately half of its mass marked by dye while the other half remains transparent. The dye tends to diffuse very slowly into the clear portion. The right side of the common line of the drop is composed of dyed glycerine, while the left side is composed of

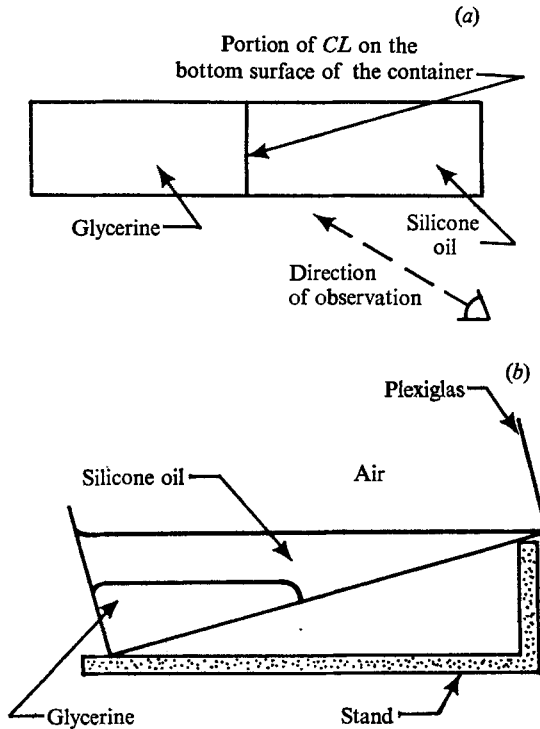


FIGURE 9. (a) Plan view of the bottom surface of the container. (b) Side view of the container of glycerine and silicone oil.

clear glycerine. The experiment proceeds by lowering the left end of the wax; see figure 7(c). After a finite length of time it is observed that the *entire* common line is composed of clear glycerine; see figure 7(d). This indicates that the dye material points, which were located on the right end portion of the common line, have moved elsewhere; on careful observation it is found that this material moves onto the glycerine–air interface.

(iii) Let F_1 be silicone oil, F_2 be glycerine and S be Plexiglas. A rectangular container made of Plexiglas is placed at an angle with respect to the horizontal; see figure 9. The container is first partially filled with glycerine and then with silicone oil. The photographs in figure 10 (plate 5) are taken from the direction indicated in figure 9 and at an angle looking down onto the bottom surface. A small amount of dye is placed on the glycerine–oil interface near the common line; see figure 10(a). The dye is composed of glycerine and McCormick’s food dye, the density of which is slightly less than that of the glycerine alone. The right end of the container is slowly lowered. It is observed that the common line moves forward (to the right) and the dye mark tends to approach the common line; see figures 10(b) and (c).

As time progresses the dye mark becomes part of the common line (figure 10 d) and finally disappears from sight; it is no longer on the glycerine–oil interface but remains adhered to the Plexiglas. Two things should be noted. (a) The shape of the mark remains roughly circular as in (i). (b) The glycerine just beneath the

interface moves forward more slowly than the material points on the interface. This is evidenced by the thinning of the dye mark at its forward position (see figure 10*c*).

(iv) The same system as in (iii) is considered. However, the common line is made to move backwards (to the left) by slowly raising the right end of the container. First a drop of dyed glycerine is deposited on the lower surface of the container, which is initially covered with silicone oil. After a few moments, the drop ‘pops’; for a side view of the fluids, see figure 11(*d*) (plate 6). The right end of the container is lowered and the clear glycerine moves forward, eventually merging with the dyed glycerine as shown in figure 11(*b*). Now the right end of the container is gradually raised (not lowered). As a consequence of the dyed glycerine being less dense than the clear part, it is seen that most of the dye appears to flow up the glycerine–oil interface. *Despite* this occurrence, the portion of the dye initially in contact with the Plexiglas remains there as shown in figure 11(*c*). As the common line moves to the left, this remaining dye comes off the bottom surface. Finally, the *entire* mark is lifted off the bottom surface as shown in figure 11(*e*). This illustrates again that material on the common line at one instant in time (the dyed glycerine) appears to move onto the fluid–fluid interface after the elapse of a *finite* interval of time.

It has been established, through the qualitative experiments, that the common line is *not* a material line (nor a material region), i.e. different fluid points are identified with the common line at different times. This is the foundation of the basic assumption which will be taken as an axiom for all analysis that follows.

3. Fluid material surfaces emitted at the moving common line

In the previous section, by means of a dye mark, it was seen that one of the displacing fluids undergoes a ‘rolling’ type motion. In this section we look at the motion of the ‘other’ fluid. It will be shown that if material points on F_1F_2 are mapped onto CL , then a material surface must be emitted from CL into the interior of F_1 which consists of F_1 material points that earlier resided on F_1S . In this instance, F_2 is undergoing the rolling motion. The system is allowed to involve unsteady flow over a deforming solid wall. In fact, the surface of the solid need not have a well-defined tangent plane at CL .

Assume the following.

(i) The basic assumption (forward).

(ii) The trajectories of the F_1 material points and the S material points located on SF_1 at \mathbf{R}_0 at $t = 0$ are given by

$$\mathbf{x}_{F_1}(t) \equiv \lim_{\substack{\mathbf{R} \rightarrow \mathbf{R}_0 \\ \mathbf{R} \in F_1}} \boldsymbol{\chi}(\mathbf{R}, t) \quad \text{for all time,} \quad (3.1a)$$

$$\mathbf{x}_S(t) \equiv \lim_{\substack{\mathbf{R} \rightarrow \mathbf{R}_0 \\ \mathbf{R} \in S}} \boldsymbol{\chi}(\mathbf{R}, t) \quad \text{for all time,} \quad (3.1b)$$

where \mathbf{R}_0 is not on CL , $\boldsymbol{\chi}(\mathbf{R}, t)$ is the deformation mapping of the material and $\mathbf{R} = \boldsymbol{\chi}(\mathbf{R}, 0)$.

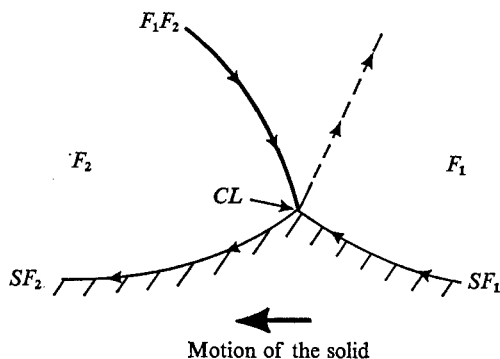


FIGURE 12. A single ejected surface in a two-dimensional motion with the frame of reference fixed to CL . The solid is shown with a dimple at CL but the analysis holds whether the solid is flat or deformed.

(iii) The mass of F_1 is conserved with no sources or sinks and with the density function $\rho \neq 0, \infty$ including its limiting values on the boundary of F_1 .

(iv) The velocity field for the entire system is Lipschitz continuous in a domain excluding any arbitrarily small neighbourhood of CL .

(v) The fluid does not slip at the solid wall.

It follows that the F_1 material points on SF_1 are first mapped onto CL and then into the interior of F_1 . The two-dimensional case is illustrated in figure 12. The arrows indicate the trajectories of material points. The solid surfaces in figures 12–15 have discontinuous tangent planes at CL . The analysis allows such a possibility but does not exclude the case of a flat surface.

Before proceeding with the demonstration it is worth commenting on the meaning of ‘no slip’ in (v). To say that a fluid does not slip on a solid surface means that a particular fluid material point in contact with a solid must never make contact with more than one solid material point, for all time. This does not preclude the possibility that at some instant the fluid point may leave the solid surface. If it happens that the velocity field is well-defined on the solid–fluid interface, then the no-slip condition reduces to the familiar condition that the velocity of the fluid must equal the velocity of the solid at the interface. However, there exists the possibility (not pathological) that the velocity field is not well-defined everywhere along the interface (see § 4). For such a case the first definition must be used. This points out the ambiguity in equating the term ‘adherence’ with ‘no slip’ (Truesdell & Noll 1960, p. 330; Coleman, Markovitz & Noll 1966, p. 57). The word adherence *seems* to say more; it seems to imply both no slip *and* the idea that the fluid material point in contact with the solid surface *remains in contact for all time* (Dussan V. 1972).

The main proof proceeds as follows. Let us follow the trajectory of an F_1 and an S material point which are both located at \mathbf{R}_0 at time $t = 0$. \mathbf{R}_0 may be any point on SF_1 not on CL . We denote their trajectories as $\mathbf{x}_{F_1}(t)$ and $\mathbf{x}_S(t)$, respectively. As a *self-consistency* check of the above five assumptions we have

$$\mathbf{x}_{F_1}(0) = \lim_{t \rightarrow 0} \lim_{\substack{\mathbf{R} \rightarrow \mathbf{R}_0 \\ \mathbf{R} \in F_1}} \boldsymbol{\chi}(\mathbf{R}, t) = \lim_{\substack{\mathbf{R} \rightarrow \mathbf{R}_0 \\ \mathbf{R} \in F_1}} \lim_{t \rightarrow 0} \boldsymbol{\chi}(\mathbf{R}, t) = \lim_{\substack{\mathbf{R} \rightarrow \mathbf{R}_0 \\ \mathbf{R} \in F_1}} \boldsymbol{\chi}(\mathbf{R}, 0) = \mathbf{R}_0$$

and likewise,

$$\mathbf{x}_S(0) = \lim_{t \rightarrow 0} \lim_{\substack{\mathbf{R} \rightarrow \mathbf{R}_0 \\ \mathbf{R} \in S}} \boldsymbol{\chi}(\mathbf{R}, t) = \lim_{\substack{\mathbf{R} \rightarrow \mathbf{R}_0 \\ \mathbf{R} \in F_1}} \lim_{t \rightarrow 0} \boldsymbol{\chi}(\mathbf{R}, t) = \lim_{\substack{\mathbf{R} \rightarrow \mathbf{R}_0 \\ \mathbf{R} \in F_1}} \boldsymbol{\chi}(\mathbf{R}, 0) = \mathbf{R}_0.$$

The first equality in either of the above equations follows from assumptions (ii) and (iv). The second, third and fourth equalities all follow from (iv). Assumptions (ii) and (iv) together with the result of the theorem of Picard–Cauchy (Ince 1956, §3.22) imply $\mathbf{x}_{F_1}(t) = \mathbf{x}_S(t)$ as long as \mathbf{x}_S is not on CL . This is consistent with (v), the no-slip condition. Since CL is *moving* we know that at some particular time t_1 (this depends on the location of \mathbf{R}_0) the solid point $\mathbf{x}_S(t_1)$ must be on CL . It follows that $\mathbf{x}_{F_1}(t) = \mathbf{x}_S(t)$ for $t < t_1$. We know that $\mathbf{x}_S(t)$ for $t > t_1$ must be located on SF_2 . Where is $\mathbf{x}_{F_1}(t)$ for $t > t_1$? There are only four possible locations of the F_1 material point for $t > t_1$.

(1) It remains attached to the same solid material point, i.e.

$$\mathbf{x}_{F_1}(t) = \mathbf{x}_S(t) \quad \text{for } t > t_1. \quad (3.2)$$

(2) It is mapped onto F_1F_2 .

(3) It remains on CL .

(4) It is mapped into the interior of F_1 .

Alternative 1 is impossible because it contradicts (iii). Indeed, a moving CL implies that there exists a time $t_2 > t_1$ such that, for some $D > 0$,

$$|\mathbf{x}_S(t_2) - \mathbf{x}_{CL}(s, t_2)| > D \quad \text{for all } s, \quad (3.3)$$

where $\mathbf{x}_S(t_2)$ is on F_2S , $\mathbf{x}_{CL}(s, t)$ is the location of CL and s is the arc length along CL . If we assume that (3.2) is correct then it follows that

$$|\mathbf{x}_{F_1}(t_2) - \mathbf{x}_{CL}(s, t_2)| > D \quad \text{for all } s.$$

However, assumption (ii) implies that for any $\epsilon > 0$ there exists an $\eta > 0$ such that

$$|\mathbf{x}_{F_1}(t_2) - \boldsymbol{\chi}(\mathbf{R}, t_2)| < \epsilon$$

for all \mathbf{R} within F_1 and satisfying the relation

$$|\mathbf{R} - \mathbf{R}_0| < \eta.$$

In physical terms this states that all the F_1 material located within a distance η of \mathbf{R}_0 at time $t = 0$ is mapped to within a distance ϵ of $\mathbf{x}_{F_1}(t_2)$ at time t_2 ; since ϵ is arbitrary, we may choose $\epsilon < D$. So we have a situation in which $\mathbf{x}_S(t_2)$ is located on F_2S by virtue of the motion of CL , $\mathbf{x}_{F_1}(t_2)$ is also located on F_2S by virtue of (3.2), and all F_1 within an η -neighbourhood of \mathbf{R}_0 at $t = 0$ *must also be located on F_2S* at $t = t_2$. This implies that a finite quantity of F_1 material has zero volume at $t = t_2$, which in turn implies that $\rho = \infty$ at CL . This contradicts assumption (v).

Alternative 2 is impossible because it contradicts assumption (i); alternative 3 is also impossible because it contradicts assumption (v). This leaves, as the only possibility, alternative 4. So it has been shown that F_1 material points originally located on SF_1 must be located in the interior of F_1 at some later time.

If the ‘forward’ basic assumption were replaced above by the ‘backward’ basic assumption, then similar conclusions would hold for F_2 rather than F_1 but

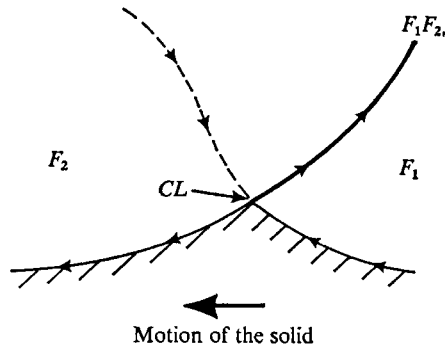


FIGURE 13. A single injected surface in a two-dimensional motion with the frame of reference fixed to CL . The solid is shown with a dimple at CL but the analysis holds whether the solid is flat or deformed.

with emitted surfaces being replaced by *injected* surfaces, i.e. the senses would be reversed in the arguments and the flow would look like that pictured in figure 13. Here a *single* injected surface is pictured although, again, several could conceivably exist (only one has been observed experimentally).

The emitted surfaces could be visualized in an experiment by marking a piece of F_1 adjacent to SF_1 . Figure 14 shows the evolution of such a neighbourhood. The material points $\{MP_i: i = 1, 2, 3, 4\}$ originally reside on SF_1 and a finite time after having passed through CL reside on the emitted surface interior to F_1 . Another emitted surface can be visualized in an experiment by marking a piece of F_1 adjacent to F_1F_2 . Figure 15 shows its evolution. Again, material points $\{MP_i: i = 1, 2, 3, 4\}$ originally on F_1F_2 pass through CL and become part of an emitted surface interior to F_1 .

Actual experiments that depict this ‘forward’ case have been performed. A schematic drawing of the apparatus is shown in figure 16. The system consists of a Plexiglas container with a rectangular base, silicone oil and a mixture of 60% water and 40% methyl alcohol. The common line formed can be moved in either direction. A drop of the alcohol–water mixture containing food dye is injected onto the interface between the Plexiglas and alcohol and water. The dye remains undisturbed for a time to allow it to diffuse very close to the wall. The end of the tank (right-hand end) containing the oil is slowly raised. Hence, F_1 is the alcohol–water mixture and F_2 is the silicone oil. CL moves towards the dye mark and when it appears to be touching it has a wedge shape. Figure 17(a) (plate 7) shows the mark before touching while figure 17(b) shows it immediately after touching.

The same experiment is performed again with a dye mark on F_1F_2 . As the dye is ejected, from a hypodermic needle, it spreads to form a disk. This probably reflects the surface-tension gradient induced by the presence of the dye. As the oil end (right hand) of the container is raised, CL moves to the left and the dye mark moves downwards toward CL . The emitted surface is clearly visible in figure 18(c) (plate 8). In this experiment the two emitted surfaces appear to coincide as pictured in figure 12.

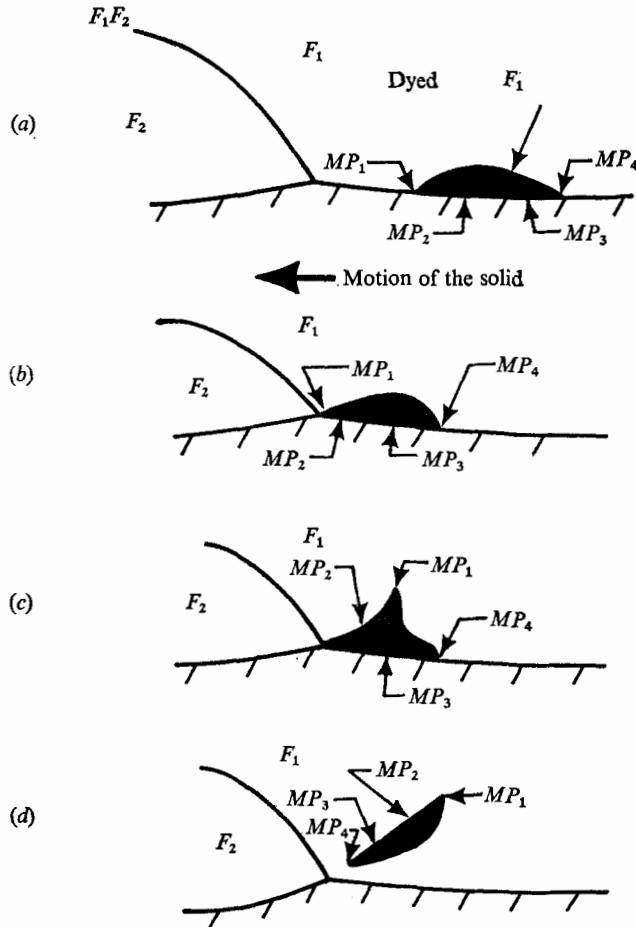


FIGURE 14. The trajectory of a dyed portion of F_1 initially in contact with the solid surface. (a) $t = t_1$. (b) $t = t_2$. (c) $t = t_3$. (d) $t = t_4$. $t_1 < t_2 < t_3 < t_4$.

The 'backward' version of the same system has been examined as well. Here CL moves toward the oil, so that the oil is F_1 . An *injected* surface in F_2 is expected. This is achieved by *lowering* the oil (right hand) end of the tank. Figure 19 depicts the evolution of a spot of dyed F_2 on the F_2 side of CL . The dye distinctly divides into two parts. This seems compatible with the existence of a *single injected* surface in F_2 .

These demonstrations should not be taken as 'experimental proof' of the validity of assumptions (i)–(v); but rather as evidence that they are self-consistent. Other models can give rise to observations similar to figures 17 and 18; refer to Dussan V. (1972, pp. 90–93).

Figures 12 and 13 resemble graphs given in Huh & Scriven (1971). In order to examine a boundary-value problem, they impose many assumptions. It is unclear which parts of their solution are realistic owing to the fact that the normal stress boundary condition is not satisfied at the fluid–fluid interface and infinite forces are predicted. The present analysis shows that the existence of emitted

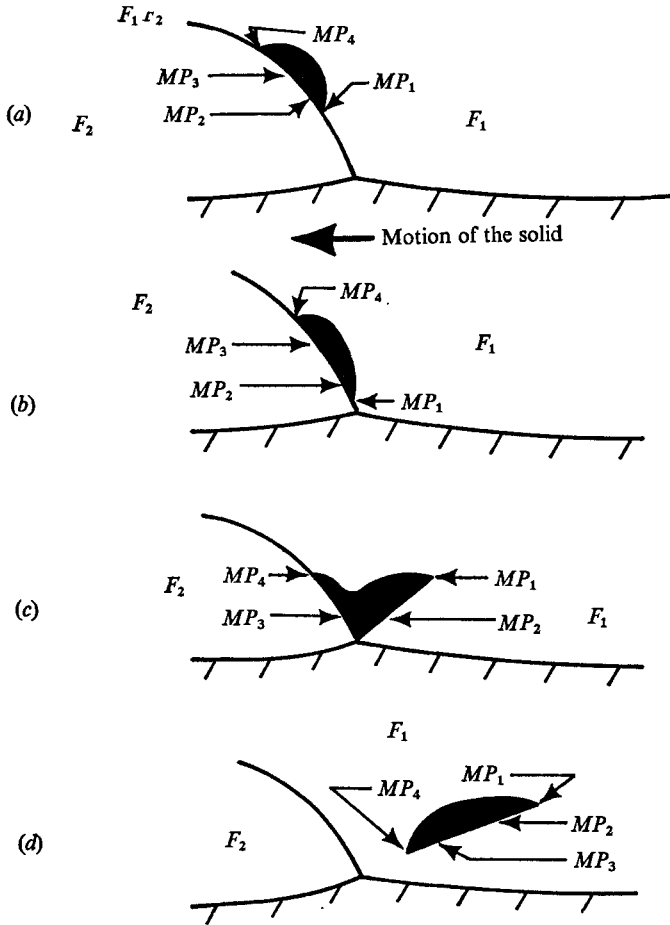


FIGURE 15. The trajectory of a dyed piece of F_1 initially in contact with the fluid–fluid interface. (a) $t = t_1$, (b) $t = t_2$, (c) $t = t_3$, (d) $t = t_4$. $t_1 < t_2 < t_3 < t_4$.

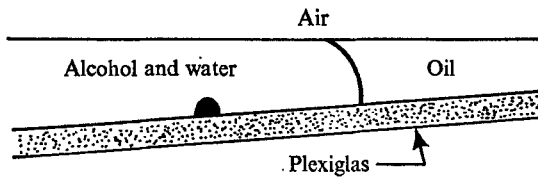


FIGURE 16. The alcohol–water and oil system with a dyed spot.

(injected) surfaces is a kinematical necessity, i.e., independent of conservation of linear momentum, and a consequence of a set of precisely stated assumptions. Huh & Scriven's analysis contains these assumptions; therefore, the resemblance in the figures is inevitable.

It has been shown that the no-slip boundary condition and a moving common line are kinematically compatible concepts.

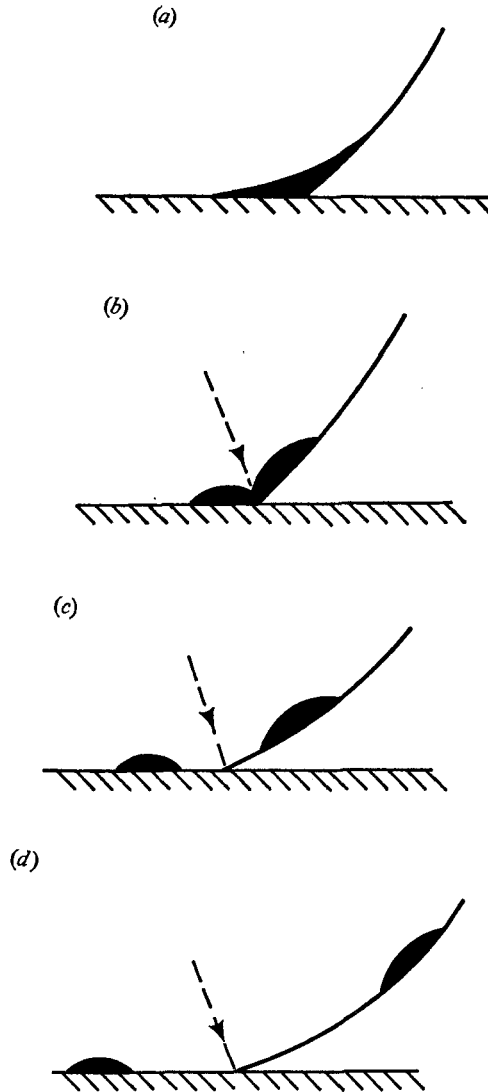


FIGURE 19. Two-dimensional illustration of the experiment. The dye mark at $t = t_1$ consists of alcohol, water and food dye. The deformation of originally one piece of alcohol and water dye as the common line moves forward the oil. An injected surface is indicated. (a) $t = t_1$. (b) $t = t_2$. (c) $t = t_3$. (d) $t = t_4$. $t_1 < t_2 < t_3 < t_4$.

4. The velocity field at CL is multi-valued

If, in addition to the assumptions of the previous section, it is assumed that (i) the solid surface is rigid and planar and (ii) $F_1 F_2$ and the ejected (injected) surface are sufficiently smooth, then the velocity field at CL is multi-valued. The important additional restriction here is that the solid be rigid; the planarity assumption is made for convenience.

Consider a rectangular Cartesian co-ordinate system that moves with CL . The origin is at CL and the solid moves past with velocity $\mathbf{U} = U\mathbf{i} + W\mathbf{k}$. The x direc-

tion is along the wall, the y direction is normal to the wall and into the fluid while the z direction lies on the wall along the local CL tangent. The unit vectors in the (x, y, z) directions are denoted by $(\mathbf{i}, \mathbf{j}, \mathbf{k})$. CL is assumed to be moving normal to itself so that $U \neq 0$. Except for isolated points, it is sufficient to assume that $U \neq 0$. The fluid velocity field is denoted by $\mathbf{u}(\mathbf{x}, t) = (u, v, w)$.

The existence of a multi-valued velocity field \mathbf{u} at $\mathbf{x} = \mathbf{0}$ can be seen by showing that the limit

$$\lim_{\mathbf{x} \rightarrow \mathbf{0}} \mathbf{u}(\mathbf{x}, t)$$

evaluated along $\{SF_i: i = 1, 2\}$, and either $F_1 F_2$ or the ejected (injected) surface differ.

Assume that either $F_1 F_2$ or an ejected (injected) surface can be represented by an equation of the form $F(\mathbf{x}, t) = 0$, where F has continuous first derivatives up to and including the boundary. This implies that the speed of propagation c and the unit normal \mathbf{n} of the surface are well-defined and are given by the following:

$$c \equiv -\frac{\partial F}{\partial t} / |\nabla F|, \quad \mathbf{n} = \nabla F / |\nabla F|.$$

In addition the following limits exist:

$$\lim_{\substack{\mathbf{x} \rightarrow \mathbf{0} \\ \mathbf{x} \in \{F=0\}}} c(\mathbf{x}, t) = c(\mathbf{0}, t), \quad (4.1 a)$$

$$\lim_{\substack{\mathbf{x} \rightarrow \mathbf{0} \\ \mathbf{x} \in \{F=0\}}} \mathbf{n}(\mathbf{x}, t) = \mathbf{n}(\mathbf{0}, t). \quad (4.1 b)$$

A material point on $F = 0$ remains on $F = 0$ as long as it is not on CL . Hence,

$$F_t + uF_x + vF_y + wF_z = 0 \quad (4.2)$$

for all non-zero \mathbf{x} on $F = 0$. A material point on $\{SF_i: i = 1, 2\}$ remains there as long as it is not on CL . Since there is no slip allowed,

$$\mathbf{u}(x, 0, z, t) = \mathbf{U} = U\mathbf{i} + W\mathbf{k} \quad (4.3)$$

for all \mathbf{x} on the solid surface, excluding CL .

It follows from (4.2) that on $F = 0$

$$\mathbf{u}(\mathbf{x}, t) = (u, -[F_t + uF_x + wF_z]F_y^{-1}, w). \quad (4.4)$$

From the definition of the co-ordinate system it follows that for all time

$$c(\mathbf{0}, t) = 0, \quad \mathbf{k} \cdot \mathbf{n}(\mathbf{0}, t) = 0. \quad (4.5 a, b)$$

Hence, from (4.1) and (4.5) it follows that

$$\lim_{\substack{\mathbf{x} \rightarrow \mathbf{0} \\ \mathbf{x} \in \{F=0\}}} c(x, t) = 0 \quad (4.5 c)$$

and

$$\lim_{\substack{\mathbf{x} \rightarrow \mathbf{0} \\ \mathbf{x} \in \{F=0\}}} \mathbf{n}(\mathbf{x}, t) \cdot \mathbf{k} = 0. \quad (4.5 d)$$

If all these facts are brought together, the two limits

$$\mathbf{L}_1 \equiv \lim_{\substack{\mathbf{x} \rightarrow \mathbf{0} \\ \mathbf{x} \in \{F=0\}}} \mathbf{u}(\mathbf{x}, t)$$

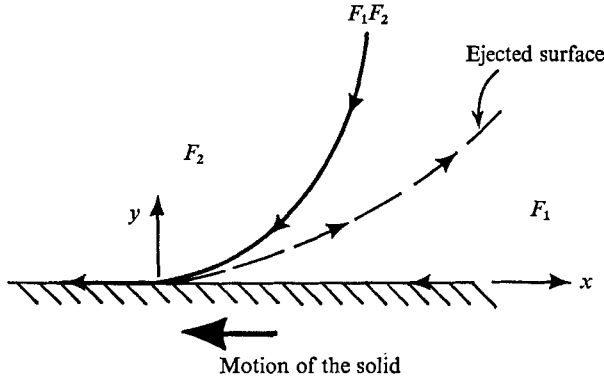


FIGURE 20. This is the motion on the x, y plane at $z = 0$.

and

$$\mathbf{L}_2 \equiv \lim_{\substack{\mathbf{x} \rightarrow \mathbf{0} \\ y=0}} \mathbf{u}(\mathbf{x}, t)$$

can be evaluated:

$$\mathbf{L}_1 = \lim_{\substack{\mathbf{x} \rightarrow \mathbf{0} \\ \mathbf{x} \in \{F=0\}}} \left(u, \frac{\mathbf{n} \cdot \mathbf{i}}{\mathbf{n} \cdot \mathbf{j}} u, w \right), \tag{4.6 a}$$

$$\mathbf{L}_2 = (U, 0, W). \tag{4.6 b}$$

There are three distinct cases to examine.

Case I. $\mathbf{n} \cdot \mathbf{i} \neq 0, \mathbf{n} \cdot \mathbf{j} \neq 0$ at $\mathbf{x} = \mathbf{0}$. This implies that the instantaneous contact angle $\theta \neq 0, \frac{1}{2}\pi, \pi$.

Take $F = 0$ as $F_1 F_2$. Equation (4.6 a) shows that the x and y components of \mathbf{L}_1 are either both zero or both non-zero. Since it is assumed that $U \neq 0$ in (4.6 b), it follows that $\mathbf{L}_1 \neq \mathbf{L}_2$.

Case II. $\mathbf{n} \cdot \mathbf{i} \neq 0, \mathbf{n} \cdot \mathbf{j} = 0$ at $\mathbf{x} = \mathbf{0}$. This implies that the instantaneous contact angle $\theta_1 = \frac{1}{2}\pi$.

Take $F = 0$ as $F_1 F_2$. The y components (4.6 a) and (4.6 b) can only be compatible if $u = 0$, in which case the x components are not. Hence, $\mathbf{L}_1 \neq \mathbf{L}_2$.

Case III. $\mathbf{n} \cdot \mathbf{i} = 0, \mathbf{n} \cdot \mathbf{j} \neq 0$ at $\mathbf{x} = \mathbf{0}$. This implies that the instantaneous contact angle $\theta_1 = 0, \pi$.

If $F = 0$ is taken to be $F_1 F_2$, it is possible for $\mathbf{L}_1 = \mathbf{L}_2$ but if $F = 0$ is taken to be the ejected (injected) surface, then $\mathbf{L}_1 \neq \mathbf{L}_2$. This situation is illustrated in figure 20.

The x component of \mathbf{L}_2 is merely U with $U < 0$. The x component of \mathbf{L}_1 along the ejected surface is necessarily non-negative. Hence, $\mathbf{L}_1 \neq \mathbf{L}_2$.

Owing to relations (4.1 b) and (4.5 d), it is impossible for both $\mathbf{n} \cdot \mathbf{i} = 0$ and $\mathbf{n} \cdot \mathbf{j} = 0$ to hold.

5. The forces exerted by the fluids in the neighbourhood of the common line

It has been shown that the basic assumption together with the no-slip condition on a rigid bounding surface necessarily give rise to a discontinuous (multi-valued) velocity field at CL . It is easily seen that this type of discontinuous velocity field

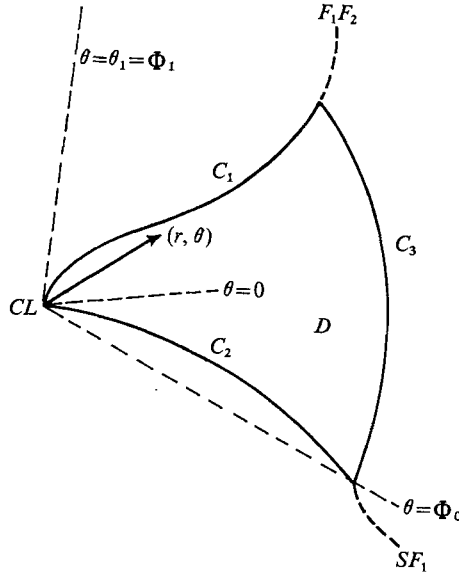


FIGURE 21. The frame of reference is at rest with respect to the common line. The angles Φ_0 and Φ_1 are defined such that for any point $(r, \theta) \in D$ we have $\Phi_0 \leq \theta \leq \Phi_1$. The angle θ_1 is between the tangent to C_1 at the common line and the tangent to C_2 at the common line. $0 < \theta_1 < \pi$.

must necessarily possess gradients that are unbounded at CL . If the fluids have constitutive relations (equations which give the explicit dependence of the stress tensor) that involve the strain rate tensor, then there exists the possibility that the stress tensor must also be unbounded at CL . This must occur, for example, if the fluids are Newtonian. An unbounded stress tensor, in itself, is not worrisome. There exist physical situations where the force distributed over a small area is replaced by a force acting at a point or a line. (This implies an unbounded stress tensor.) This can make good sense in that the mathematical model can predict values of physically measurable quantities, such as the displacements, velocities and forces, which agree well with experiment. However, it is also possible that an unbounded stress tensor may give rise to an *unbounded force*. Such a mathematical theory then may be considered *physically unrealistic*, at least near the singularity.

In this section the forces exerted by incompressible fluids undergoing two-dimensional steady motion will be examined. The velocity field is assumed to be (a) discontinuous at the common line (as a result of §4) and (b) representable in a given general form. The result is that an integral $I(\eta)$ is unbounded. When the fluid is Newtonian, $I(\eta)$ is the tangential component of the *force* exerted by the fluid on a planar surface that lies totally within the fluid and extends up to CL .

Consider a bounded domain, shown in figure 21, which lies totally within one of the fluids, say F_1 . Its bounding curve C consists of three piecewise smooth curves $\{C_i: i = 1, 2, 3\}$ having the following properties.

- (a) C_1 is a part of F_1F_2 that includes CL .

(b) C_2 is a part of SF_1 that includes CL . The instantaneous contact angle θ_1 is restricted to the range $0 < \theta_1 < \pi$.

(c) C_3 is any single-valued smooth curve joining those end points of C_1 and C_2 that are not on CL .

θ is the angle between the tangent to C_2 at CL and a position vector from CL . The radial and azimuthal velocity components are denoted by u and v respectively.

If (i) the fluid is incompressible, (ii) the motion is steady and two-dimensional, and (iii) the fluid velocity field is representable in a certain general form (see the appendix), then, for any $\eta > 0$, there exists an angle θ_* , $0 < \theta_* < \theta_1$, for which the integral

$$I(\eta) = \int_0^\eta \left[\frac{\partial v}{\partial r} - \frac{1}{r}v + \frac{1}{r} \frac{\partial u}{\partial \theta} \right]_{\theta=\theta_*} dr \quad (5.1)$$

is *unbounded*.

The details of the representation are given in the appendix but the main feature to be found there is the inclusion of a discontinuity in u at CL . The necessity for such a discontinuity was shown in §4.

It is convenient to express u and v in the following form:

$$u(r, \theta) = f(\theta) + V_1(r, \theta), \quad (5.2a)$$

$$v(r, \theta) = g(\theta) + V_2(r, \theta), \quad (5.2b)$$

where
$$(f(\theta), g(\theta)) \equiv \lim_{\substack{r \rightarrow 0 \\ \theta \text{ fixed}}} (u(r, \theta), v(r, \theta)) \quad (5.2c)$$

and
$$(f(0), g(0)) = \lim_{\theta \rightarrow 0} (f(\theta), g(\theta)). \quad (5.2d)$$

Now, since u is multi-valued at $r = 0$, it follows from assumption (A 8b) that

$$f(0) \neq f(\theta_1). \quad (5.2e)$$

V_1 and V_2 are subject to certain smoothness assumptions. The incompressibility condition

$$r \frac{\partial u}{\partial r} + u + \frac{\partial v}{\partial \theta} = 0$$

can be written in terms of representation (5.2) in the form

$$g' + f + r \frac{\partial V_1}{\partial r} + U + \frac{\partial V_2}{\partial \theta} = 0. \quad (5.3)$$

These derivatives exist as a consequence of assumptions (A 2) and (A 4). If θ is fixed in $(0, \theta_1)$ and the limit $r \rightarrow 0$ is taken in (5.3), assumptions (A 2) and (A 9) guarantee the following limiting form:

$$g' + f = 0, \quad 0 < \theta < \theta_1. \quad (5.4)$$

Since f is at least $C^{(1)}$ in $[0, \theta_1]$ by assumptions (A 2) and (A 4), then g' is well-defined there as well. These assumptions, furthermore, allow a differentiation of (5.4):

$$g'' + f' = 0, \quad 0 < \theta < \theta_1. \quad (5.5)$$

Consider now the expression $I(\eta)$ given in (5.1). In terms of representation (5.2), it becomes

$$I(\eta) = \int_0^\eta \left[\frac{1}{r} \left(f' - g + \frac{\partial V_1}{\partial \theta} - V_2 \right) + \frac{\partial V_2}{\partial r} \right]_{\theta=\theta_*} dr. \quad (5.6)$$

V_2 is assumed to be absolutely continuous in r for fixed θ , so that the Radon–Nikodym theorem (Riesz & Sz-Nagy 1955, p. 137) implies that

$$V_2(r, \theta) = \int_0^\eta \frac{\partial V_2}{\partial r} dr.$$

Hence, the contribution to $I(\eta)$ due to

$$\int_0^\eta \frac{\partial V_2}{\partial r} dr$$

is finite. Consequently, in order for the integral $I(\eta)$ to be finite for all $0 \leq \theta_* \leq \theta_1$, it is necessary that

$$f' - g + \partial V_1 / \partial \theta - V_2 = o(1) \quad \text{as } r \rightarrow 0$$

along a ray. By definition of V_2 and assumption (A 7) it follows that

$$f' - g = 0, \quad 0 \leq \theta \leq \theta_1, \quad (5.7)$$

must hold.

If f' is eliminated between (5.5) and (5.7), then

$$g'' + g = 0, \quad (5.8a)$$

with

$$g(0) = g(\theta_1) = 0. \quad (5.8b)$$

This last expression is merely the alternative form of assumption (A 8a). As long as $0 \leq \theta \leq \theta_1 < \pi$ the only solution of system (5.8) is

$$g(\theta) \equiv 0$$

and so through (5.4),

$$f(\theta) \equiv 0, \quad 0 \leq \theta \leq \theta_1.$$

However, this contradicts the multi-valuedness (5.2e) of the u velocity component. Hence there must exist an angle θ_* , $0 \leq \theta_* \leq \theta_1$, in which $I(\eta)$ is unbounded for any $\eta > 0$.

If it could be proved that *all* solutions to the Navier–Stokes equations must possess velocity fields with the structure described, then one would know for Newtonian fluids that the following statements are physically incompatible because they give rise to infinite forces: (i) the no-slip condition on the rigid bounding surface, (ii) the basic assumption. However, this is a formidable task. The less general problem of the fluid in the neighbourhood of the common line undergoing Stokes flow (i.e. a two-dimensional ‘slow’ motion of two incompressible Newtonian fluids) has been considered. The resulting stream functions which represent the velocity field obey the biharmonic equation. No assumptions need be made concerning the jump conditions at the interface. It was shown (Dussan V. 1972) that, if there exists a solution to the biharmonic equation in a finite domain containing parts of the two fluids surrounding the common line and if the velocity field, evaluated on the boundary of this finite domain, is

sufficiently smooth (except at the common line), then *at least one of the fluids exerts an infinite force on the solid bounding surface*. It is the multi-valued velocity field at the common line which gives rise to the infinite force.

6. Discussion and conclusions

A continuum model of the kinematics of the materials near a moving common line has been presented. The class of motions analysed is described by the basic assumption. The basic assumption states that in a finite time material points on the fluid–fluid interface arrive at the common line or else leave the common line and arrive on the fluid–fluid interface. In essence, the basic assumption is a formalization of the concept of ‘rolling’. If points arrive at the common line from the fluid–fluid interface and then remain adhered to the solid, then the interfacial motion is reminiscent of a moving tractor tread. Rolling has been previously mentioned in the literature in connexion with a bolus of mercury moving through a capillary tube and a drop moving down an inclined plane (Yarnold 1938; Schwartz, Rader & Huey 1964). However, even though it is very instructive to think of rolling little use has been made of these observations.

The basic assumption sharply distinguishes the common-line region from a neighbourhood of a stagnation point. In the latter case, the velocity field is analytic at the stagnation point, so that material points on the dividing streamline take an infinite time to arrive there.

It was shown that the basic assumption, together with common fluid mechanical assumptions, requires that the flow field must have certain properties. As little mechanical structure as possible was imposed on the flow near the common line so as to make as transparent as possible the *raison d'être* for these properties. No mention need be made of the mathematical model of an interface, i.e. a surface of zero thickness *vs.* a thin but finite layer. More important, no interfacial jump conditions are imposed. *The derived properties* are independent of *such concepts as surface tension, surface viscosity or elasticity, concentration of surface-active material, disjoining pressures*, etc. In addition the balance of linear momentum is not invoked. Hence, no constitutive assumption on the fluids is necessary and the conclusions hold for non-Newtonian as well as Newtonian fluids. This might be especially important near the interfaces and common line if these are viewed as having finite thickness since then the properties would likely be non-Newtonian.

It has been shown theoretically that at least one *fluid material surface must be emitted* (injected) from a moving common line into (from) the *interior* of one of the displacing fluids. The fluid that constitutes these surfaces originates on the fluid–solid boundary and on the fluid–fluid interface. This has been shown to follow from the no-slip boundary condition, the basic assumption, and conservation of mass. This also illustrates that the no-slip boundary condition is kinematically compatible with a moving common line.

It has been shown that the velocity field must be multi-valued at the moving common line. This followed directly from the basic assumption, the no-slip boundary condition, and the wall being considered rigid.

It has been shown that the integral $I(\eta)$ must be unbounded for two-dimensional, incompressible steady flow as long as the velocity field has a certain amount of specified structure. The multi-valuedness at the common line is, of course, essential. If the fluids in question were Newtonian, $I(\eta)$ would represent the tangential component of the force exerted by the fluid on a plane within the fluid and intersecting the common line. The unboundedness of $I(\eta)$ would, then, imply the existence of infinite forces (this may also follow for certain classes of non-Newtonian fluids, e.g. Stokesian fluids).

It is this last property that is most distressing. It strongly indicates that the cause of the singularities that others previously referenced have been getting in their solutions lies in their *model* and *not* in the fact that exact solutions were not obtained. The basic model must be reconsidered. What can be done to relieve the force singularity? It is already known that changing the boundary conditions on the fluid–fluid interface will not work. One possibility is to seek a non-Newtonian description of the local properties of the bulk fluids near the common line. The integral $I(\eta)$ might then represent a quantity different from the force and hence its unboundedness might be tolerable. The analysis makes clear that *any contrivance* that relieves the multi-valuedness of the velocity field at the common line simultaneously relieves the singularity in $I(\eta)$. Hence, *any* slip coefficient will do the job. It is therefore essential that the solutions of posed boundary-value problems containing slip coefficients be able to predict some measurable physical quantities before the imposed slip is taken as a reasonable description of the local boundary condition. There are a variety of possibilities (see Huh & Scriven 1971) for the elimination of the singularity each one of which entails detailed solutions of well-posed boundary-value problems.

The authors gratefully acknowledge the support of the National Science Foundation, Engineering Mechanics Program through grant GK 31794.

Appendix. Details of assumptions of §5

The following assumptions are made on $u = u(r, \theta)$ and $v = v(r, \theta)$.

(A 1) u and v are bounded in D .

(A 2) u and v are $C^{(3)}$ in $D - C(\epsilon)$ for any $\epsilon > 0$, where $C(\epsilon)$ denotes an ϵ -neighbourhood about the origin.

(A 3) For any *fixed* θ in the interval $[\Phi_0, \Phi_1]$, the functions u and v are absolutely continuous functions of r (see Riesz & Sz-Nagy 1955). It can easily be shown that the above assumptions imply the existence of two bounded functions $f(\theta)$ and $g(\theta)$, where

$$f(\theta') \equiv \lim_{\substack{r \rightarrow 0 \\ \theta = \theta'}} u(r, \theta), \quad g(\theta') \equiv \lim_{\substack{r \rightarrow 0 \\ \theta = \theta'}} v(r, \theta)$$

for $0 < \theta < \theta_1$. For certain geometries of D there exists the possibility that the functions f and g are well-defined over the *closed* interval $0 \leq \theta' \leq \theta_1$. The functions $V_1 = V_1(r, \theta)$ and $V_2 = V_2(r, \theta)$ are defined for all $(r, \theta) \in D \{0 < \theta < \theta_1\}$ as follows:

$$V_1(r, \theta) \equiv u(r, \theta) - f(\theta), \quad V_2(r, \theta) \equiv v(r, \theta) - g(\theta).$$

(A 4) $\partial V_1/\partial\theta$ and $\partial V_2/\partial\theta$ exist and are $C^{(1)}$ in $\{D - C(\epsilon)\} \{0 < \theta < \theta_1\}$ for any $\epsilon > 0$.

(A 5) The limits of f and g as $\theta \rightarrow \theta_1$ and $\theta \rightarrow 0$ exist (finite) and are defined as $f(\theta_1), f(0), g(\theta_1)$ and $g(0)$, where

$$\begin{aligned} f(\theta_1) &= \lim_{\substack{\theta \rightarrow \theta_1 \\ \theta < \theta_1}} f(\theta); & f(0) &= \lim_{\substack{\theta \rightarrow 0 \\ \theta > 0}} f(\theta); \\ g(\theta_1) &= \lim_{\substack{\theta \rightarrow \theta_1 \\ \theta < \theta_1}} g(\theta); & g(0) &= \lim_{\substack{\theta \rightarrow 0 \\ \theta < 0}} g(\theta). \end{aligned}$$

(A 6) The following equalities hold:

$$\begin{aligned} f(\theta_1) &= \lim_{\substack{r \rightarrow 0 \\ (r, \theta) \in C_1}} u(r, \theta); & f(0) &= \lim_{\substack{r \rightarrow 0 \\ (r, \theta) \in C_2}} u(r, \theta); \\ g(\theta_1) &= \lim_{\substack{r \rightarrow 0 \\ (r, \theta) \in C_1}} v(r, \theta); & g(0) &= \lim_{\substack{r \rightarrow 0 \\ (r, \theta) \in C_2}} v(r, \theta). \end{aligned}$$

$$(A 7) \quad \lim_{\substack{r \rightarrow \theta \\ \theta = \theta'}} \partial V_1/\partial\theta = \partial\{\lim_{\substack{r \rightarrow 0 \\ \theta = \theta'}} V_1\}/\partial\theta \quad \text{for } 0 < \theta' < \theta_1.$$

By definition of V_1 , $\lim_{\substack{r \rightarrow 0 \\ \theta = \theta'}} V_1 = 0$. Hence, this assumption can be written as

$$\lim_{\substack{r \rightarrow 0 \\ \theta = \theta'}} \partial V_1/\partial\theta = 0 \quad \text{for } 0 < \theta' < \theta_1.$$

Likewise,

$$\lim_{\substack{r \rightarrow 0 \\ \theta = \theta'}} \partial V_2/\partial\theta = \partial\{\lim_{\substack{r \rightarrow 0 \\ \theta = \theta'}} V_2\}/\partial\theta \quad \text{for } 0 < \theta' < \theta_1.$$

By definition of V_2 , it follows that

$$\lim_{\substack{r \rightarrow 0 \\ \theta = \theta'}} \partial V_2/\partial\theta = 0 \quad \text{for } 0 < \theta' < \theta_1.$$

(A 8a) $\mathbf{u} \cdot \mathbf{n} = 0$ on C_1 and on C_2 not including the origin. The vector \mathbf{n} is perpendicular to the tangent vectors \mathbf{t} of the curves C_1 and C_2 . The boundary curves are considered smooth with well-defined tangents as $r \rightarrow 0$ so we have that

$$\lim_{\substack{r \rightarrow 0 \\ (r, \theta) \in C_1}} \mathbf{u} \cdot \mathbf{n} = \lim_{\substack{r \rightarrow 0 \\ (r, \theta) \in C_1}} v$$

and

$$\lim_{\substack{r \rightarrow 0 \\ (r, \theta) \in C_2}} \mathbf{u} \cdot \mathbf{n} = \lim_{\substack{r \rightarrow 0 \\ (r, \theta) \in C_2}} v.$$

As a consequence of assumption (A 8a) it follows that

$$\lim_{\substack{r \rightarrow 0 \\ (r, \theta) \in C_1}} v = 0, \quad \lim_{\substack{r \rightarrow 0 \\ (r, \theta) \in C_2}} v = 0.$$

Using assumption (A 6) an *alternative form for assumption* (A 8a) can be written:

$$g(\theta_1) = 0, \quad g(0) = 0.$$

(A 8b)

$$\lim_{\substack{r \rightarrow 0 \\ (r, \theta) \in C_1}} \mathbf{u} \cdot \mathbf{t} \neq \lim_{\substack{r \rightarrow 0 \\ (r, \theta) \in C_2}} \mathbf{u} \cdot \mathbf{t}.$$

This gives a discontinuous velocity at the common line. Using assumption (A 6) an *alternative form for assumption (A 8b)* can be written:

$$f(\theta_1) \neq f(0),$$

where the geometry is restricted so that $0 < \theta_1 < \pi$.

$$(A\ 9) \quad \lim_{\substack{r \rightarrow 0 \\ \theta = \theta_1}} (r \partial V_1 / \partial r) = 0 \quad \text{for } 0 < \theta' < \theta_1.$$

It can be shown for a neighbourhood of $r = 0$ on $\theta = \theta'$ that if $\partial V_1 / \partial r$ is monotonic without bound or if $\partial V_1 / \partial r$ is bounded, then

$$\lim_{\substack{r \rightarrow 0 \\ \theta = \theta'}} (r \partial V_1 / \partial r) = 0 \quad \text{for } 0 < \theta' < \theta_1.$$

REFERENCES

- BASCOM, W. D., COTTINGTON, R. L. & SINGLETERRY, C. R. 1964 In *Contact Angles, Wettability and Adhesion* (ed. R. F. Gould), pp. 355–379. Washington: Am. Chem. Soc.
- BENSON, G. C. & YUN, K. S. 1967 *Solid–Gas Interface* (ed. E. A. Flood), vol. 1. Marcel Dekker.
- COLEMAN, B. D., MARKOVITZ, H. & NOLL, W. 1966 *Viscometric Flows of Non-Newtonian Fluids*. Springer.
- DUSSAN V., E. B. 1972 Ph.D. thesis, Dept. Mech. & Mat. Sci., The Johns Hopkins University, Baltimore, Maryland.
- HANSEN, R. J. & TOONG, T. Y. 1971 *J. Colloid Interface Sci.* **37**, 196.
- HUH, C. & SCRIVEN, L. E. 1971 *J. Colloid Interface Sci.* **35**, 85.
- INCE, E. L. 1956 *Ordinary Differential Equations*. Dover.
- LUDVIKSSON, V. & LIGHTFOOT, E. N. 1968 *A.I.Ch.E. J.* **14**, 674.
- LUDVIKSSON, V. & LIGHTFOOT, E. N. 1971 *A.I.Ch.E. J.* **17**, 1166.
- MAXWELL, J. C. 1876 Capillary action. *Encycl. Brit.* 9th edn. London. (See also 11th edn.)
- MOFFATT, H. K. 1964 *J. Fluid Mech.* **18**, 1.
- PRUTOW, R. J. & OSTRACH, S. 1971 *AFOSR Sci. Rep.* no. 70-28827, FTAS/TR-70-56.
- READ, W. T. & SHOCKLEY, W. 1950 *Phys. Rev.* **78**, 275.
- RIESZ, F. & SZ-NAGY, B. 1955 *Functional Analysis*. New York: Unger.
- SCHONHORN, H., FRISCH, H. L. & KWEI, T. K. 1966 *J. Appl. Phys.* **37**, 4967.
- SCHWARTZ, A. M., RADER, C. A. & HUEY, E. 1964 In *Contact Angles, Wettability and Adhesion* (ed. R. F. Gould), pp. 250–267. Washington: Am. Chem. Soc.
- TRUESDELL, C. A. & NOLL, W. 1960 *Classical Field Theories, Handbuch der Physik*, vol. 3/1. Springer.
- WORTHINGTON, A. M. 1963 *A Study of Splashes*. Macmillan.
- YARNOLD, G. D. 1938 *Proc. Phys. Soc.* **50**, 540.
- ZISMAN, W. A. 1972 *J. Paint Tech.* **44**, 41.

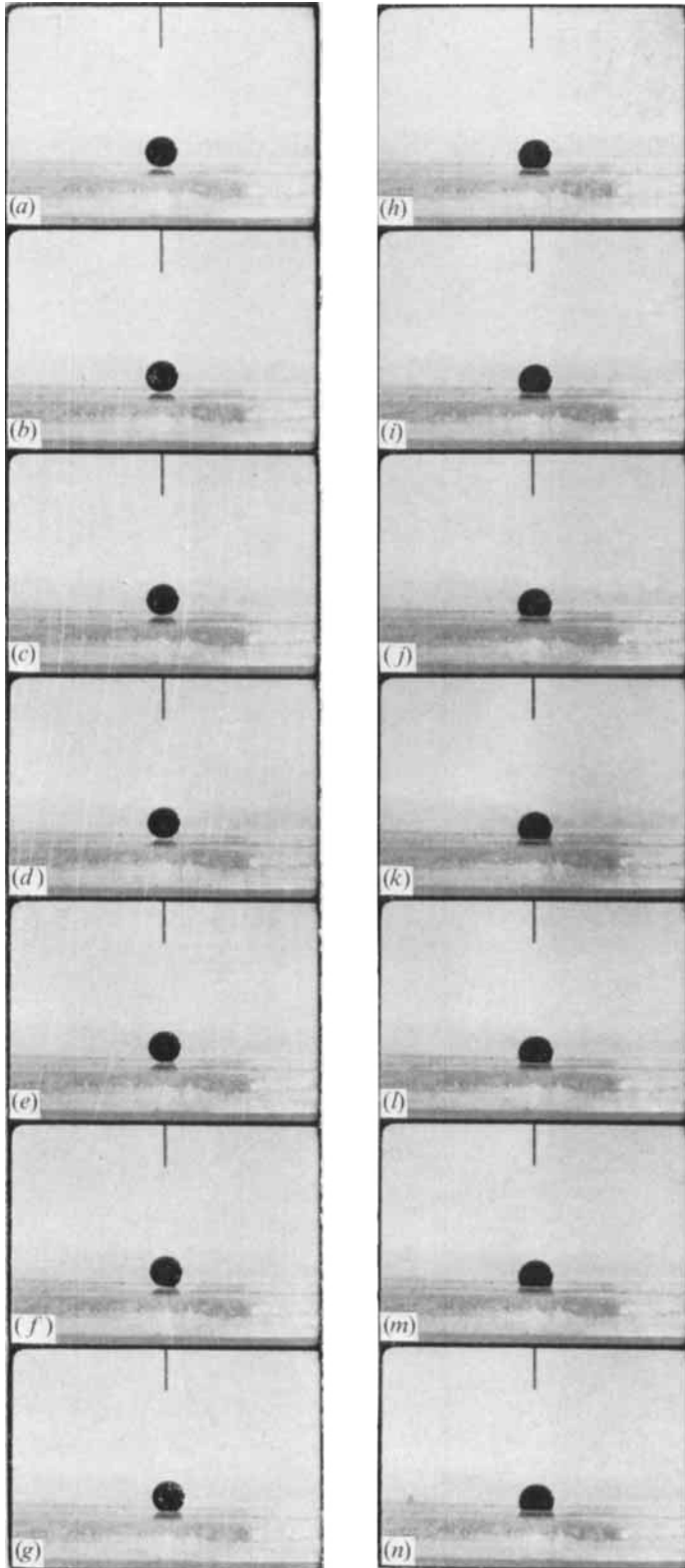


FIGURE 2. A drop of water containing food dye is released from a hypodermic needle. The drop is surrounded by silicone oil ($\nu = 10$ centistokes). The bottom surface is Plexiglas.

The drop 'popped' in less than 0.75 s. The motion picture was taken at 18 frames/s.

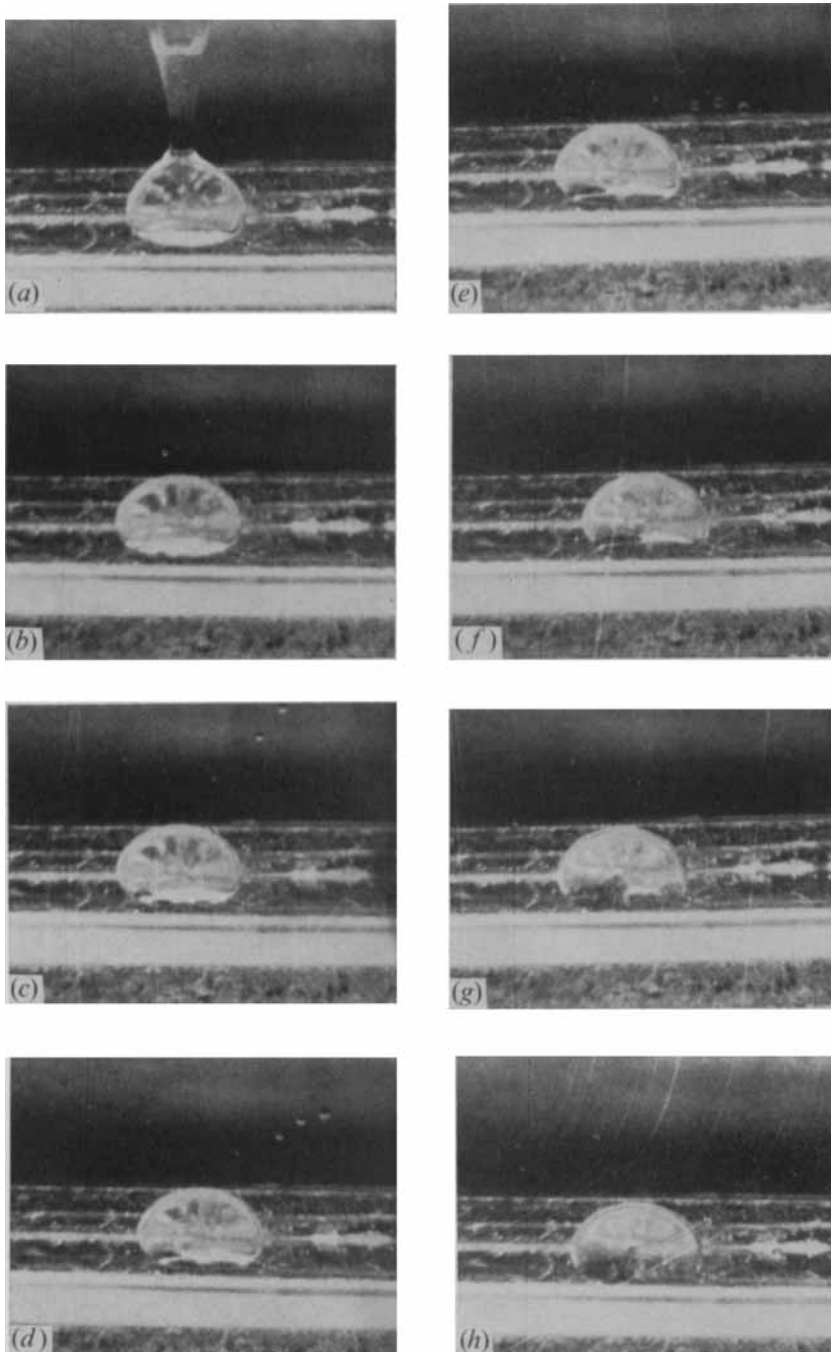


FIGURE 3. Glycerine drop surrounded by silicone oil 'popping' on a Plexiglas surface.

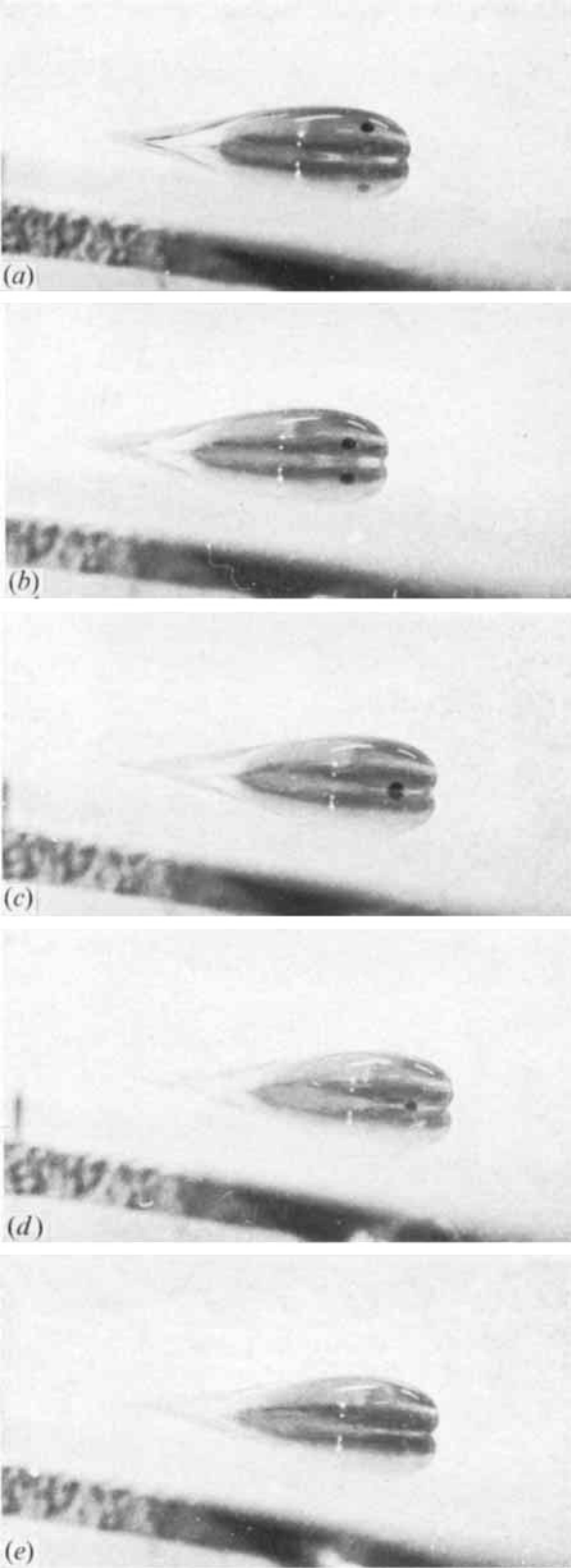


FIGURE 5. A drop of honey moving on a Plexiglas surface.
DUSSAN V. AND DAVIS

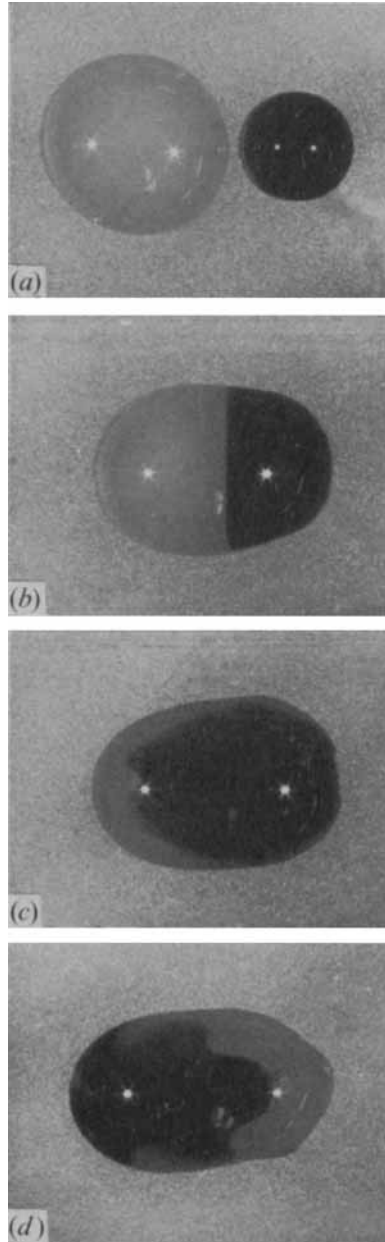


FIGURE 7. (a) Two drops of glycerine on a bee's wax surface. (b) Now there is *one* drop, part of which is dyed. The arrows beneath (c) and (d) indicate the direction of movement of the drop of glycerine.

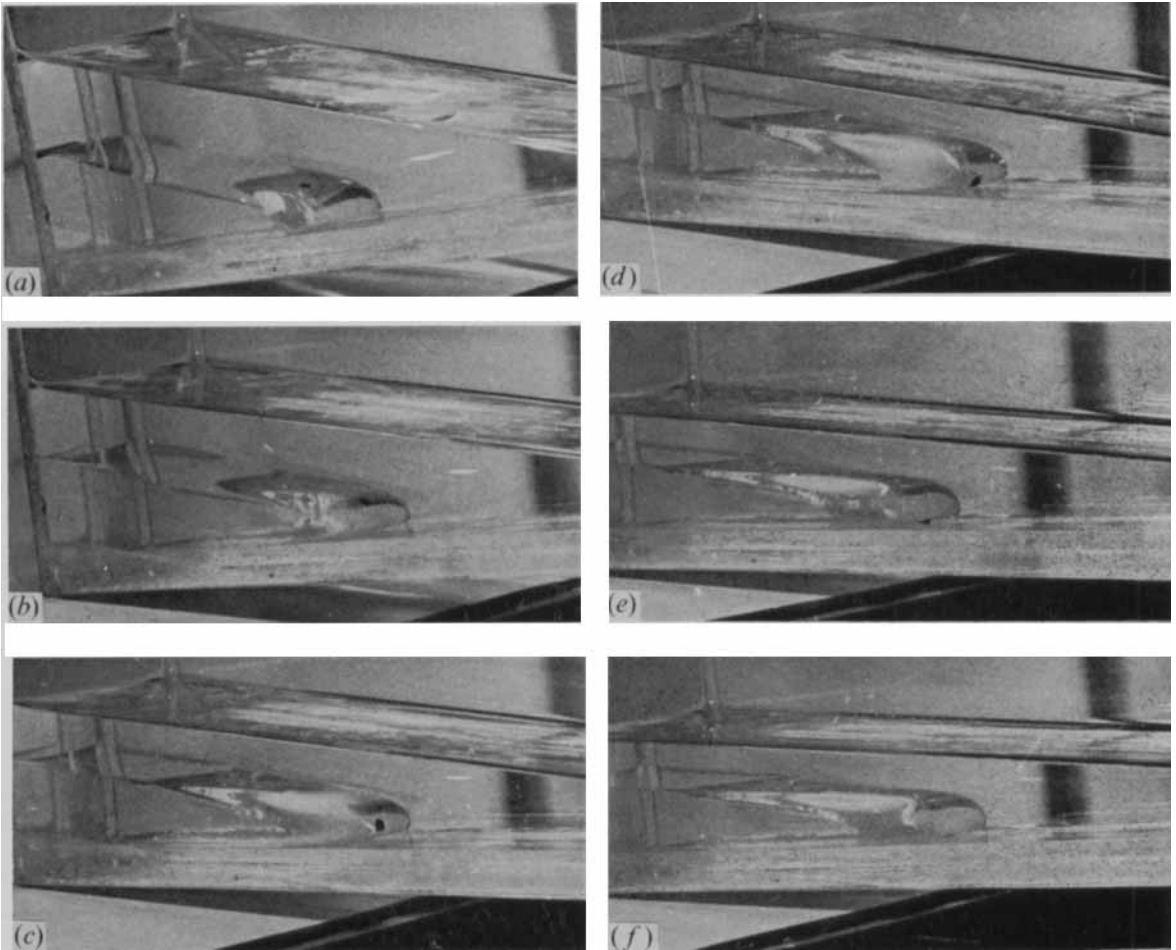


FIGURE 10. The motion of a dyed piece of glycerine on the glycerine–oil interface.
The glycerine is the lower fluid, and the oil is the upper fluid.

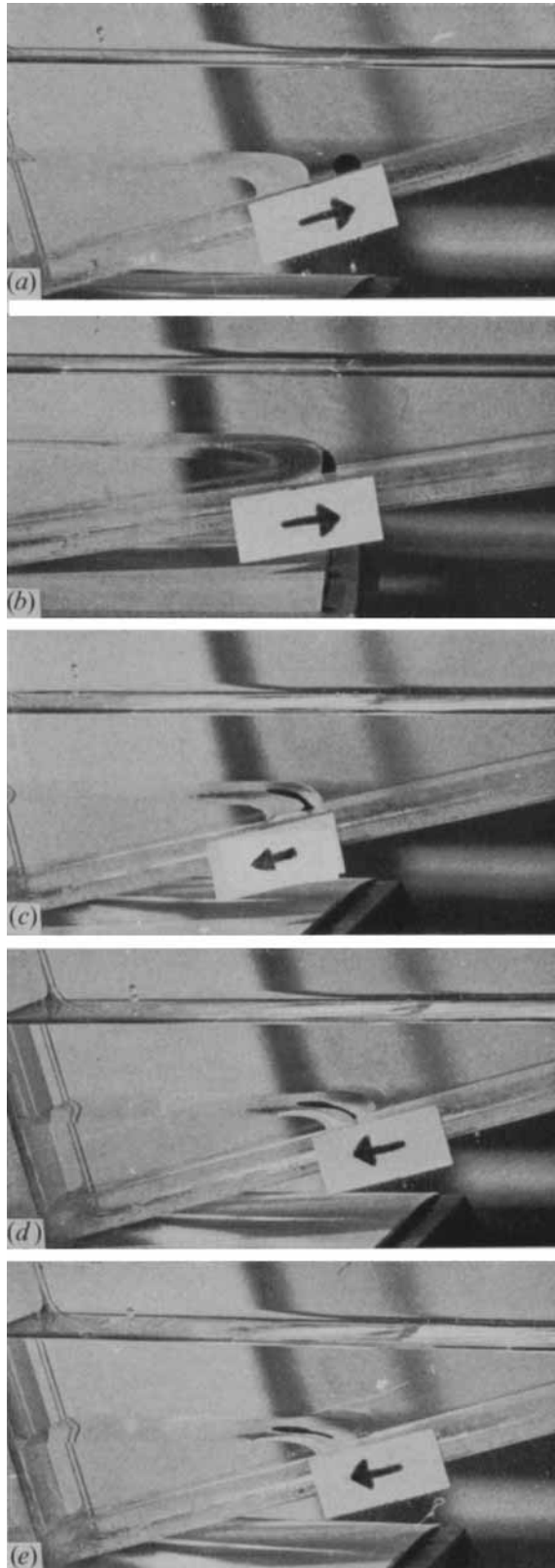


FIGURE 11. The lower fluid and the dyed fluid are composed of glycerine. The upper fluid is oil. The arrows indicate the direction of motion of the common line.

DUSSAN V. AND DAVIS

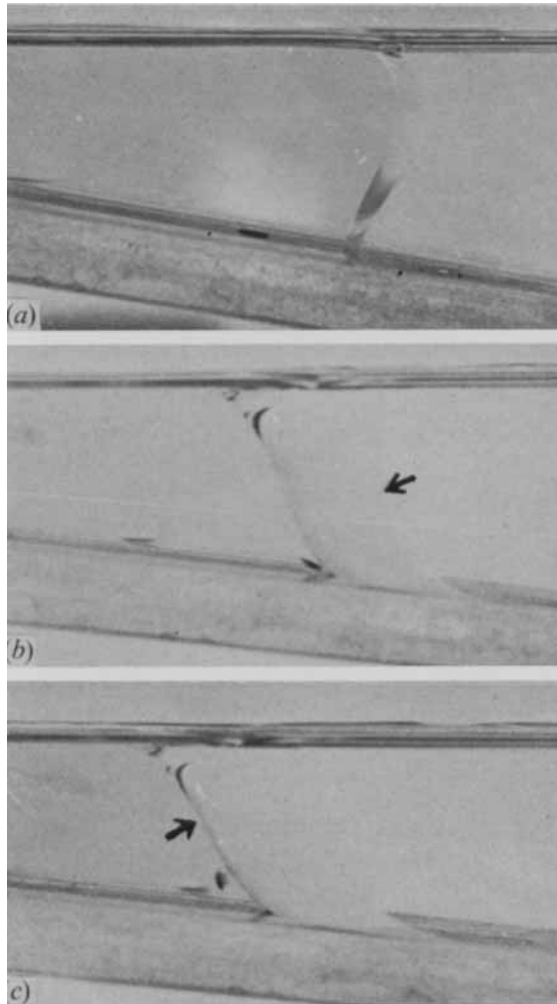


FIGURE 17. The fluid–fluid interface in (a) is relatively flat, i.e. perpendicular to the page. In (b) and (c) the interface bends. The arrow in (b) points to the location of the common line on the front face of the container. The arrow in (c) points to that portion of the fluid–fluid interface which is located midway between the front and back of the container. The portion of the dye facing the interface in (c) appears ‘fuzzy’ owing to the fact that the dye is bent; consequently in (c) we are observing only its outer edges.

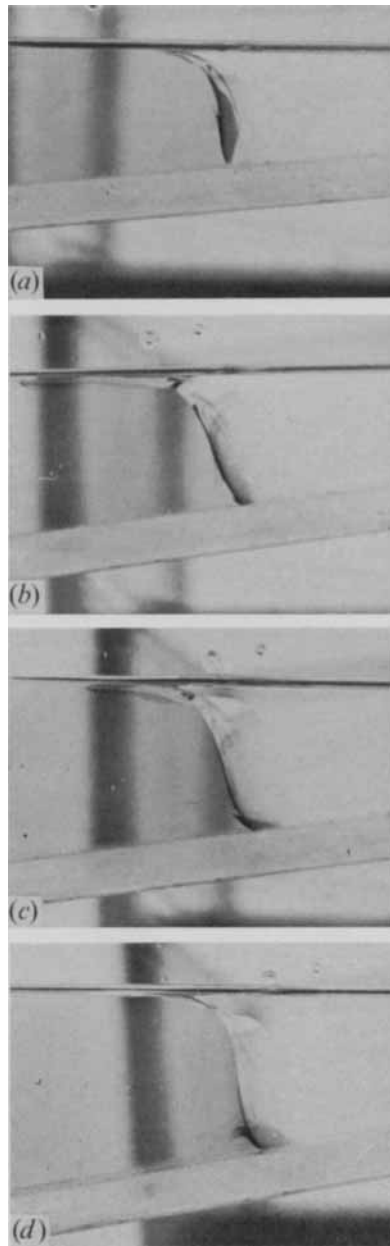


FIGURE 18. Owing to the bend in the interface, we can see only half of the 'disk' like initial configuration of the dye in (a). In (b) we begin to see the emitted surface. Again, owing to the bend in the fluid-fluid interface, the bottom side of the emitted surface is quite distinct in (c) at the location midway between the front and rear of the container. At positions closer to the front of the container, the emitted surface of dye looks like a dark curtain rising from the bottom of the fluid-fluid interface, as shown in (c) and (d).